Engineering and Technology Journal
Journal homepage: https://etj.uotechnology.edu.iq

The influence of micro channel on the performance of low concentrator parabolic collector systems with phase change material

Jenan D. Hamdi *, Jalal M. Jalil, Ahmed H. Reja

Electromechanical Engineering Dept., University of Technology-Iraq, Alsina'a street, 10066 Baghdad, Iraq.
*Corresponding author Email: eme.20.05@grad.uotechnology.edu.iq

HIGHLIGHTS

- A new receiver and reflector design was used in the parabolic solar concentrator
- The reflector focuses solar radiation on two sides
- Tracking maintained the parabolic collector's perpendicular sun alignment
- The maximum energy storage period was 3 hours

ARTICLE INFO

Handling editor: Sattar Aljabair

Keywords:
Thermal energy storage; Microchannels; latent heat; solar concentrator; Two-axis tracking; Paraffin wax

ABSTRACT

Increasing global economic development leads to a continuous increase in energy demand, considering the limited conventional resources of energy as well as the impact on the environment associated with its use. The primary disadvantage of solar energy is that it is only accessible during the day. Thermal energy storage systems can overlook this flaw since they can store energy throughout the day for use at night. This paper presents a new cooling technique for low-concentration parabolic collectors with microchannel and Phase Change Material (PCM). A test model consisting of a parabolic concentrator was designed and fabricated to test the parabolic concentrator with and without PCM in Baghdad city during January, March, and July. The solar receiver is an essential component of a solar-powered system and was manufactured from Aluminum metal with 44 microchannels (0.3 m in length, 0.02 m in width, and 0.009 m in height), where the receiver consisted of four rows of microchannels, each row consisting of 11 channels is constructed with velocity and temperature measurement facilities to achieve the experimental results. The results show that the PCM will store the energy roughly three hours after sunset at a flow rate of 0.009339 kg/s. Also, the result indicated that the two-axis tracking system would increase thermal efficiency.

1. Introduction

Due to the continued increase in greenhouse gas emissions and fluctuation in fuel prices, we must adapt to renewable energy sources and use energy more voluntarily. Solar energy has received a lot of interest since it is abundant and sustainable, but its intermittent nature precludes it from being widely employed [1]. On the other hand, solar energy storage has been widely demonstrated to be an effective technology for boosting system flexibility, enhancing solar thermal energy utilization efficiency, and lowering heating costs. The primary disadvantage of solar energy is that it is only accessible during the day [2,3]. Thermal energy storage systems can overlook this flaw since they can store energy throughout the day for use at night. Paraffin wax was considered a significant substance that could store energy through a phase change [4-6]. On the other hand, microchannel technology can improve solar collectors' performance and thermal efficiency. A technique to enhance heat transfer is to raise the heat transfer coefficient through recirculation and vortex generation by adding microstructures and cavities along the flow path [7,8]. The potential of Microchannel Heat Sink (MCHS) to provide high heat flux cooling must be fully realized through the optimization of microchannel design. Many studies [9,10] have been done on this topic to optimize the micro-channel design for optimal heat transfer performance in small areas. For this reason, it is widely known that microchannel cooling technology, which operates at a high heat transfer coefficient within a small space, offers several benefits to thermal-fluid systems.

Al Ghuol et al. [11] designed, analyzed, and constructed a single-pass solar air heater with an approach PCM. The temperature fluctuated between 30°C and 35°C during the testing for the solar collector with spherical capsules as a PCM, and the air mass flow rate varied between 0.03 and 0.09 kg/s. The experimental result shows that the thermal storage efficiency of the built-in solar air heater attained a maximum value of 71% at 0.05 kg/s mass flow rate, its charging time dropped by about

http://doi.org/10.30684/etj.2024.144040.1619
Received 05 November 2023; Received in revised form 20 December 2023; Accepted 10 January 2024; Available online 05 February 2024
2412-0758/University of Technology-Iraq, Baghdad, Iraq

70%, and its cooling rate rose with the usage of paraffin wax-aluminum composite. Murtadha et al. [12] tested a room with specific dimensions, and Solar Chimneys (SC) were installed on a wall facing south with Aspect Ratios (AR) greater than 12.

The SC collector is made of paraffin wax as a phase change material supported by a copper foam matrix to improve the combined thermal energy storage box. The collector was protected from the outside by two double-transparent acrylic panels. Thermal Energy Storage Box (TESB) is supported by a system of evacuated tubular collectors that use thermosyphons to store heat effectively. According to experimental work completed on January 25 and February 26, employing TESM in closed-loop SC throughout the day and extending its effect into the night is beneficial. The test room's heating system reached the highest room temperature just after sunset when the difference in temperature between the inside and external air was roughly 15°C. Abed et al. [13] improved the solar air heater's thermal behavior and storage efficiency by integrating cylindrical capsules into the solar air collector system. The 600 mm long, 50 mm wide cylindrical capsule is suspended in the airstream's cross flow. Three cases are tested for both natural convection and forced convection at various mass flow rates (0.5, 1.132 kg/min) under constant incident irradiation of 1000 W/m^2: cylindrical capsules packed with pure sand are used in the first case; cylindrical tablets filled with compound (sand + 10% PCM) are used in the second case; and cylindrical capsules packed with combination (sand + 20% PCM) are used in the third case. The results of the experiment demonstrated that in comparison to pure sand, the compound (sand + 20 percent PCM) offers the best thermal storage duration (380 min), with an increase in outlet air temperature of roughly 5.6% when forced convection is applied at (0.5 kg/min) (240 min). Sand plus 20% PCM results in an output air temperature increase of roughly 9.2% over pure sand and a compound (1.132 kg/min forced convection) thermal storage duration of 355 minutes (220 min).

Yang et al. [14] performed experimental and numerical investigations on a microchannel with different pin fins with rhombus, hydrofoil, and sine shapes, with areas of 0.0625 and 1061119 mm^2 overall. It was discovered through numerical simulation that sine-type pin fins produce many superior outcomes at a flow rate of 100 ml/min and a heat flux of 144 W/cm^2 compared to the others. Similarly, utilizing sine-type pin fins for a maximum velocity of 4.46 m/s results in a minor pressure loss of 15 kPa. A microchannel with a rectangular ribbed sinusoidal cavity was numerically analyzed by Ghani et al. [15] with Reynolds values ranging from 100 to 800. Research that considered the Nusselt number and friction factor was carried out. It was contended sinusoidal cavities with rectangular ribs produce better-combined output than cavities and ribs of other designs because of the greater surface area and intriguingly lower friction factor. The best results for heat transmission were obtained with a Reynolds number of 800. Jalil and Abdulkadhim [16] studied the effect of micro-channel technology on the effectiveness of solar air collectors by using numerical and experimental methods. The absorber plate is made from aluminum metal with 30 rectangular micro-channels (0.9 mm in length, 0.004 mm in width, and 0.0008 mm in height). The absorber plate also included facilities for measuring velocity, temperature, and differential pressure. Airflow of 0.0019, 0.0029, 0.0044, and 0.0053 kg/s and irradiance of 200, 400, 600, and 800 W/m^2 are the numerical and experimental parameters investigated. The result shows that the highest air temperature at the exit of the microchannel is 72.5°C.This paper explores the negative availability of solar radiation during the daytime and the lack of benefit from solar panels at sunset. This problem was addressed using energy storage materials during the day and returning the energy at sunset. Several studies on PCM material are available, but none described using PCM material with microchannels in parabolic solar concentrators. This study attempts to fill these gaps by evaluating the effect of integrating thermal energy storage systems directly with the microchannels of solar concentrators. Also, to increase the efficiency of these energy-storing materials, PCM material inside the tank contains pin fins to enhance thermal conductivity.

2. Thermal energy storage methods

The energy storage systems aim to transform Energy into a form that can be kept and used as needed by using materials that can store thermal energy when their temperature rises and release it when the temperature falls. Thermal energy storage systems are one sustainable energy storage system. Three techniques for storing thermal energy are still being researched [17,18].

- Sensible Heat Storage (SHS)
- Latent Heat Storage (LHS)
- Thermo-chemical energy storage.

2.1 Sensible heat storage (SHS)

In TES systems, thermal Energy can be stored as sensible or latent heat. Sensible Heat Storage (SHS) systems use the heat capacity that the material gains as its temperature rises to store energy. The specific heat capacity of the material, the quantity of the material, and the temperature change gradient all affect how much energy SHS systems can store. The amount of heat can be calculated by Equation (1) and Equation (2) [19]:

$$q = \int_{Ti}^{Tf} mc_p dT \quad (1)$$

$$q = mc_p(dT_f - dT_i) \quad (2)$$

2.2 Latent heat storage (LHS)

Latent heat storage (LHS) is based on phase change of material. After a specific temperature, a phase change occurs, and solid transformation into liquid occurs. The temperature will be constant until the solid material is converted into liquid. This procedure involves heating the substance till it changes phases. Phase change causes a significant amount of energy to become trapped inside the material, referred to as the latent heat of vaporization or fusion. When the temperature of phase change material

increases, its heat is first released in its initial phase (solid). The substance absorbs a significant quantity of energy during this change. Once the transition is complete, the liquid material's temperature rises again, and energy is appropriately stored. The amount of stored Energy can be calculated by Equation (3) and Equation (4) [20]:

$$q = \int_{Ti}^{Tm} mc_p dT + ma_m \Delta h_m + \int_{T_m}^{T_i} mc_p dT \quad (3)$$

$$q = m[c_{sp}(T_m - T_i) + a_m \Delta h_m + c_{Ip}(T_f - T_m) \quad (4)$$

2.3 Thermo chemical energy storage

The Energy is stored and released in thermochemical energy storage systems while completely reversible chemical reactions break or reconstruct molecular bonds. In this instance, the amount of chemical material and endothermic heat of the reaction determines the amount of heat storage [21].

Paraffin wax was a significant substance that could store energy through a phase change. Compared to numerous cycles of latent TES operation without degradation, these have very high stability. Hence, paraffin waxes were viable PCM options [22]. The widespread use of paraffin wax in latent heat thermal energy storage can be attributed to its advantageous properties, which include safety, non-interaction with other materials, harmony with materials used to make containers, high latent heat, low or no supper cooling, chemical stability, and a range of phase change temperatures. The wax's thermal properties are given in Table 1.

Table 1: Thermal properties of Paraffin wax [23]

Melting temperature (°C)	Density ($kg.m^{-3}$)	Thermal conductivity ($W.m^{-1}.K^{-1}$)	Specific heat ($J.g^{-1}.K^{-1}$)	Latent heat ($kJ.kg^{-1}$)
42	880	0.13	1.8	174.12

3. Mathematical modeling of the parabolic trough solar concentrator

The following geometric relationships between the parabolic reflector, rectangular receiver, and sun incidence angle determine the design parameters. The concentration ratio describes a particular collector's ability to concentrate a certain amount of light Energy. The geometric Concentration Ratio (CR) may be determined directly using the formula in Equation (5):

$$CR = \frac{A_a}{A_r} \quad (5)$$

The optical axis forms the rim angle (r) and the line extending from the focus point to the collector rim (also known as the focal distance or focal length), as shown in Figure 1. The best rim angle for a reflector is between 70 and 110 degrees. The rim angle is given in Equation (6):

$$\emptyset_r = \sin^{-1} \frac{W_a}{2 \times r_r} \quad (6)$$

4. Calculations thermal efficiency

Measuring the mass flow rate and the temperature difference between the air inlet and outlet from the receiver is necessary to compute the convection heat transfer shown in Equation (7) [24]:

$$q = m \cdot C_p (T_{aout} - T_{ain}) \quad (7)$$

The thermal efficiency of solar collector can be calculated by using Equation (8):

$$\eta_{th} = \frac{\dot{m} c_p (T_o - T_i)}{I A_c} \quad (8)$$

5. Experimental setup

The parabolic concentrator system used here for hot air is based on the solar radiation concentration by reflected surface. The model is locally designed, constructed, and tested. The concentrator system mainly consists of collectors (reflectors), a rectangular receiver (absorber), a blower, a control circuit, a support structure, and a rim angle equal to 90°. The reflector's structure has a rectangular shape. The reflector is 200 cm in width, 30 cm in length, and 0.5 cm in height. Aluminum is used in the reflector's manufacturing to achieve lightweight and good reflectivity.

A solar power receiver is the system's heart that transforms solar radiation into heat energy. A new design was manufactured for the receiver, where the receiver consisted of two plates of 30 * 30 cm of Aluminium with a thickness of 6 mm. These plates were drilled on both sides with a width of 20 mm and a depth of 0.9 mm. After drilling it from both sides, the plate's final shape, where notice the formation of channels. These panels are perforated from the channel in the middle and side to install the thermocable. The micro-channel is covered with two plates that are similar in dimensions and manufactured from Aluminium. The dimensions of the plate covers are 30*30*0.15 mm to ensure minimum heat resistance and the perfect thermal connection at the right micro-channel. The cover with the smoothness of the surface of each part was prepared, and the front or back was prepared to conform to the total denture manufactured in the entry and exit from the micro-channel. The receiver consists of 44

microchannels distributed between two plates. Each plate consists of 22 channels distributed in two rows. The absorber plates were painted with matte black paint, similar to the paint used to paint grills because it can withstand high temperatures without damage. The wax tank was manufactured tightly to ensure it did not leak when it reached the melting point. The wax tank dimensions are 30* 30* 4 cm, filled with paraffin wax. The tank contains 36 fins to increase heat conduction to and from the PCM; each fin has a diameter of 6 mm and a pitch equal to 4.4 cm. Figure 1 shows the recipient layers, where (a) shows the cross-section of the reciver components and (b) shows the reciver layers.

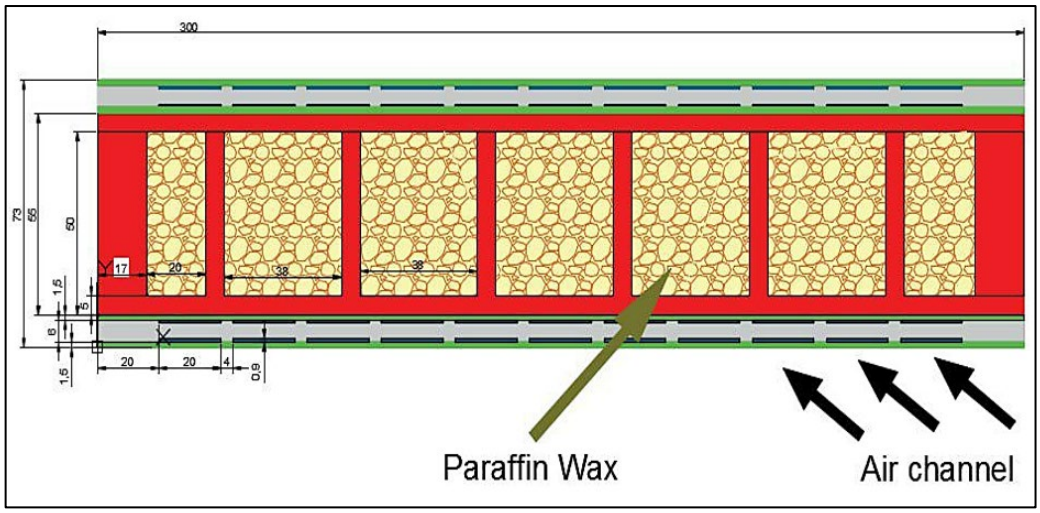

(a)

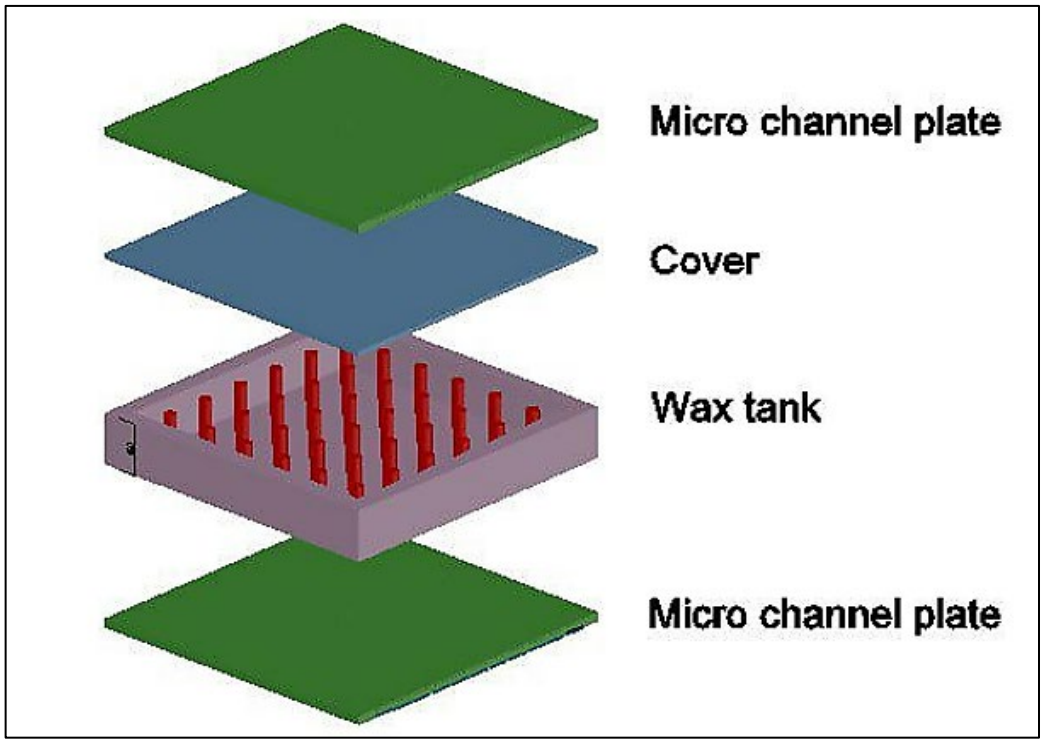

(b)

Figure 1: The receiver of the parabolic collector **(**a) Cross-section of a receiver (b) Make up the receiver

The solar air collector's cover is made of glass windows with measurements of 30 cm in length, 30 cm in breadth, and 6 mm in thickness to reduce heat losses from the receiver by convection and radiation. The centrifugal fan is an electrical apparatus for transporting air. Due to the microchannel's smallness, a high-speed blower is required to draw air flowing through these channels at varying airspeeds using a mechanical valve at the outlet air. A tracking mechanism needs to be dependable and capable of monitoring the sun with a given level of accuracy, returning the thermal collector to its starting point at the end of the day, and tracking the sun's path through clouds. Figure 2 shows tracking the sun with two axes. Figure 3 shows the photograph of the experimental apparatus.

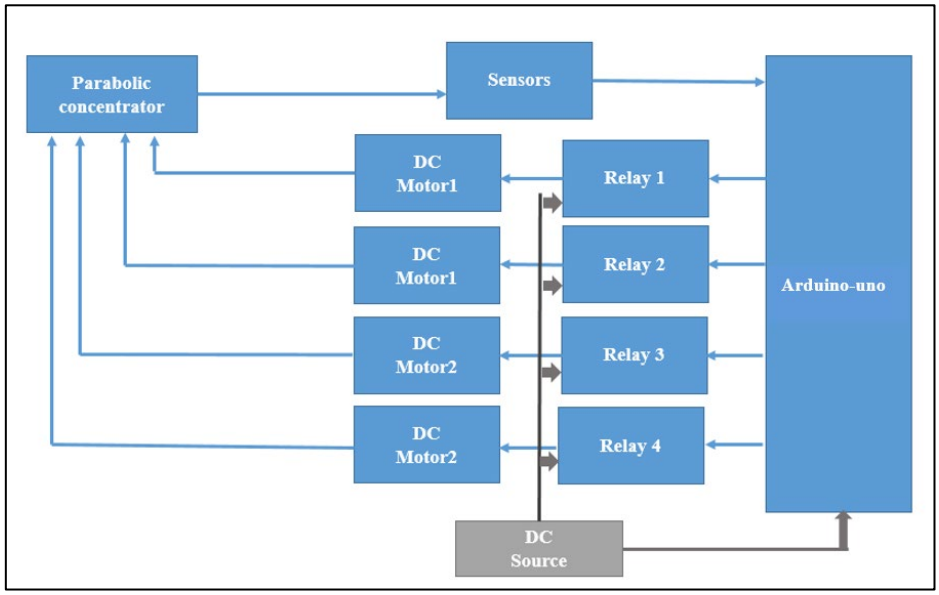

Figure 2: Block diagram of two-axis tracker

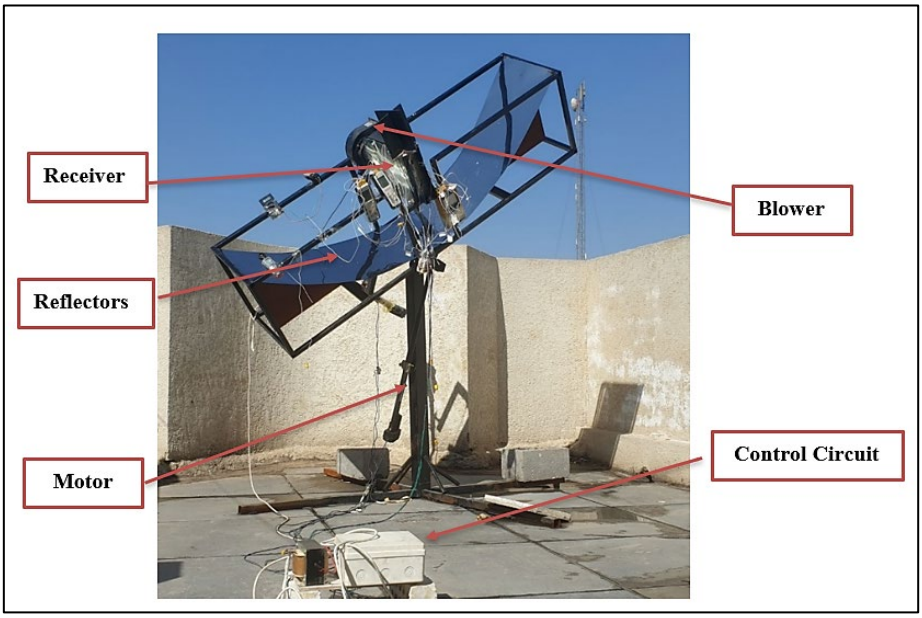

Figure 3: Photograph of the experimental apparatus

6. Results and discussion

In this section, the experimental results are interpreted and presented. The measurements were recorded between 9:00 am and 7:00 pm. All the readings have been recorded on clear days in January, March, and July 2023 at Baghdad, Iraq (latitude 33.31° and longitude 44.36°). The variation of solar radiation and ambient air temperature versus time is presented in Figures 4 and 5, respectively. The hourly variation of incident solar radiation refers to the changes in the amount of solar energy received at a particular location over a day. Several factors influence the hourly variation of solar radiation, including the time of day, season, latitude, weather conditions, and local geographical features. Solar radiation exhibits a diurnal (daily) variation due to the rotation of the Earth. The highest solar radiation occurs around noon when the sun is at its highest point in the sky; therefore, the value of solar radiation increases gradually from the morning until it reaches its maximum value at midday and then begins to decrease. The ambient temperature variation is also similar to the solar radiation profile. In July, the maximum received solar radiation was 928 W/m^2 at 13:00, and the maximum measured ambient air temperature was 47°C at 14:00.

Figure 6 shows the variation of the absorber plate temperature with the time of day at different mass flow rate values.It appears that the behavior of the absorber plate temperature with time resembles that of solar irradiance with time. In March, the maximum value of the absorber plate temperature was 78.5°C at 0.009339 kg/s airflow. The temperature of the absorber plate surface is higher than the others (inlet and outlet air temperature and glass temperature); the temperature of the absorber varies between 78.5°C at 0.009339 kg/s (minimum airflow) and 68.43°C at 0.030235 kg/s (maximum airflow). This high absorber temperature value led to using a parabolic concentrator with a concentration ratio equal to 3. The solar concentrator is designed to focus the solar radiation on two sides. Hence, the value of the solar radiation reaching the absorber plate is high, so the temperature of the absorber plate will rise.

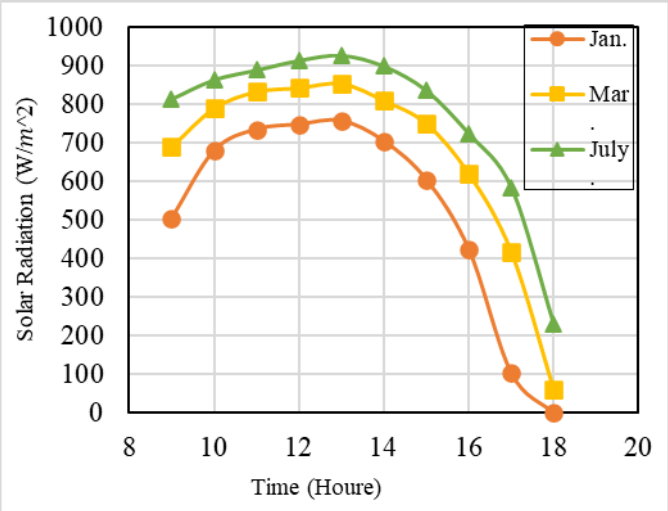

Figure 4: Hourly variation of incident solar radiation on January 16th March 17th and July 17th from 9:00 to 18:00

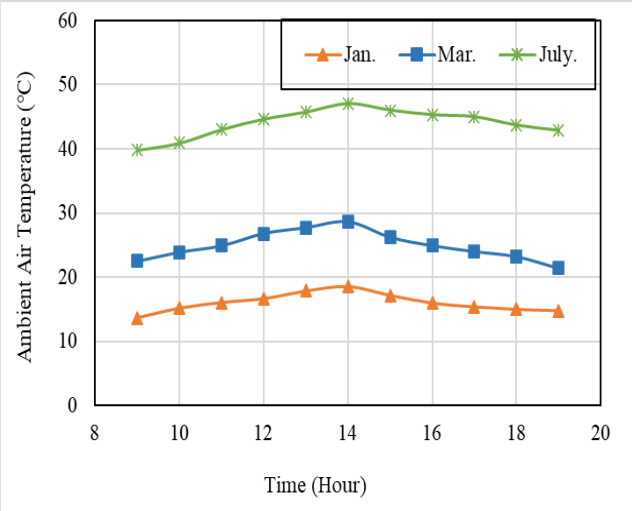

Figure 5: Hourly variation of ambient air temperature on January 16th March 17th and July 17th from 9:00 to 19:00

Also, Figure 6 shows that the surface temperature remained high even after the sunset, and this is due to the presence of paraffin wax. Figure 7 displays the solar collector's instantaneous efficiency during the daytime without PCM in the two scenarios with and without tracking. From this Figure, it is noted that the efficiency of the solar collector during 1:00 pm for the non-tracking system reaches 62.2%. In contrast, using the tracking system, the efficiency value surpasses 81.6%. This means an increase of about 23.8% when using a tracking system for solar collectors compared to a fixed system case. The resulting increase in thermal efficiency is because solar tracking makes solar radiation perpendicular to the receiver, and thus, the amount of radiation reaching the receiver is high. Therefore, the temperature of the absorber is high, and because of the presence of channels inside the absorber, the thermal energy acquired by the air is high. The Figure also shows that the thermal efficiency gradually increases until 1:00 pm. At this point, it starts to decline due to a decrease in solar radiation falling on the solar collector, which lowers the energy captured.

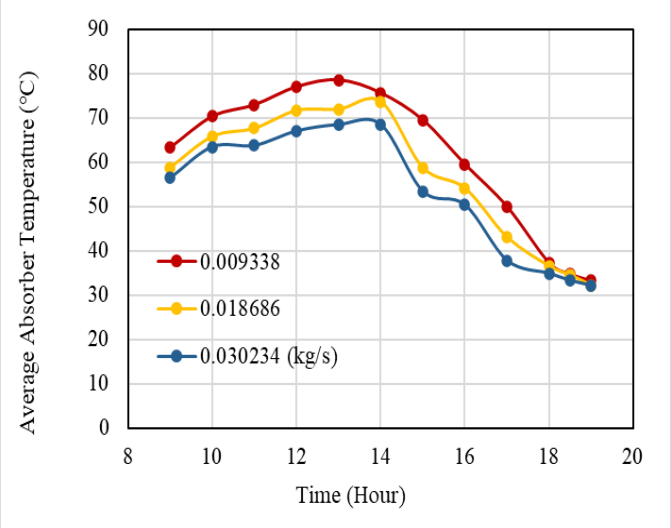

Figure 6: Hourly variation of the measured average plate temperature with PCM in March

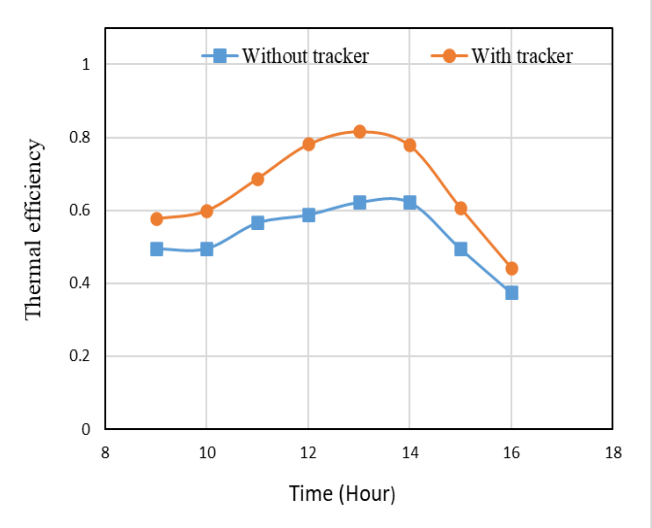

Figure 7: Hourly variation of the measured average plate temperature with PCM in March

Figure 8 illustrates the effect of inlet flow rate on thermal efficiency. The figure shows that thermal efficiency increases with increasing mass flow rate. When the flow mass increases, the thermal energy benefits from it will increase, thus increasing thermal efficiency. Also, the figure shows that the thermal efficiency is 54.98% in January, 69.3% in March, and 80.9% in July at the flow rate of 0.026064 kg/s. This high value of efficiency is due to the use of the new design of the absorbing surface. The absorber receives high-intensity solar radiation from two sides, which significantly increases the temperature of the absorbing surface. The multi-layered micro-channels inside the receiver extract the high temperature generated on the receiver because a large surface area exposed to fluid increases heat transfer from the absorber to the liquid. Since the efficiency depends on the value of the heat absorbed, the solar concentrator's thermal efficiency is high.

Figure 9 shows the effect of mass flow rate on the air temperature difference (exit–inlet) through the multi-layer of the microchannel in March. It can be seen that the maximum temperature difference occurs between 12:00 and 1:00 pm due to an increase in the solar intensity. The figures show an inverse relationship between the airflow rate and the air temperature difference because the increase in the mass flow rate means an increase in the speed of the air flowing inside the small channels, and

therefore, the air does not have enough time to absorb all the heat from the microchannel, and this leads to reduce the temperature exit. Therefore, the temperature difference will be reduced.

Figure 10 shows the change in thermal efficiency over time during March with solar tracking and variable mass flow rate; the figure shows that thermal efficiency is directly proportional to the mass flow rate. This is because increasing the mass flow rate causes an increase in the amount of heat useful, as the amount of heat useful is directly proportional to the mass, and since thermal efficiency depends on the amount of heat useful, thermal efficiency increases. Figure 11 showed (for air mass flow rates of 0.018686kg/s and a wide range of solar radiation collected for March) the variations in air temperature over time increased radiation led to an increase in the difference in air temperature. This temperature increase can be compared to the difference between paraffin wax's presence and absence. It can be observed that the solar collector continued to function for three hours after sunset, with various air temperatures depending on how much air was flowing through the solar collector. This is an example of the effect of adding a phase-changing material as a heat storage medium.

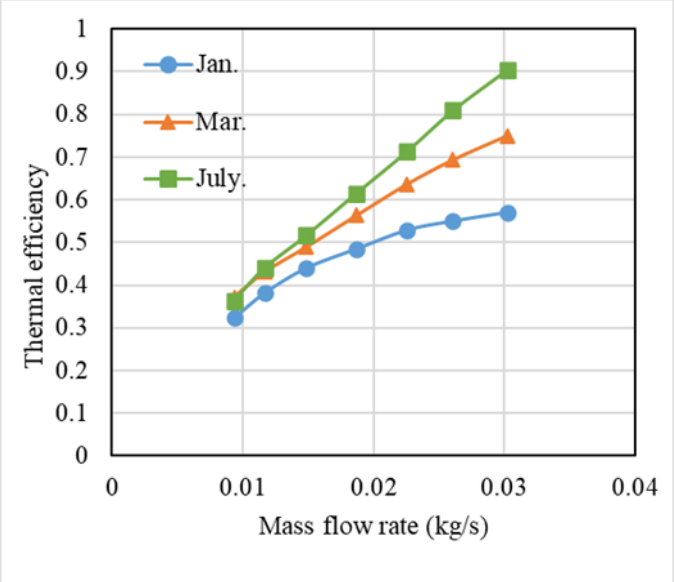

Figure 8: The effect of inlet flow rate on thermal efficiency on January 16 March 17th and July 17th at 1:00 pm

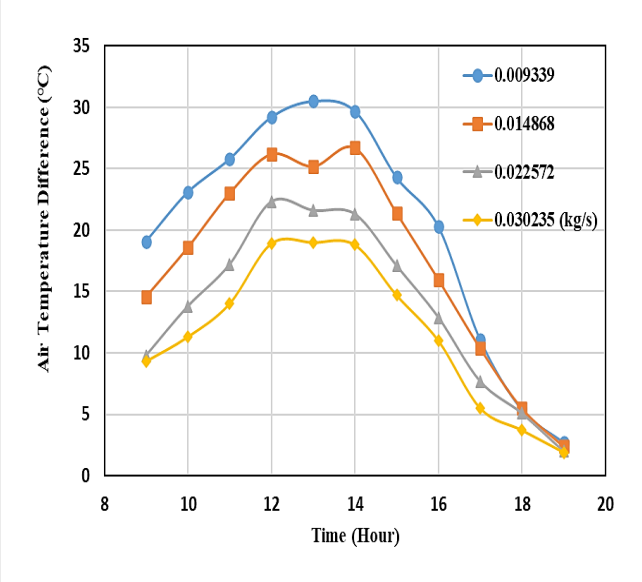

Figure 9: Time-dependent variation of air temperature difference with PCM in March

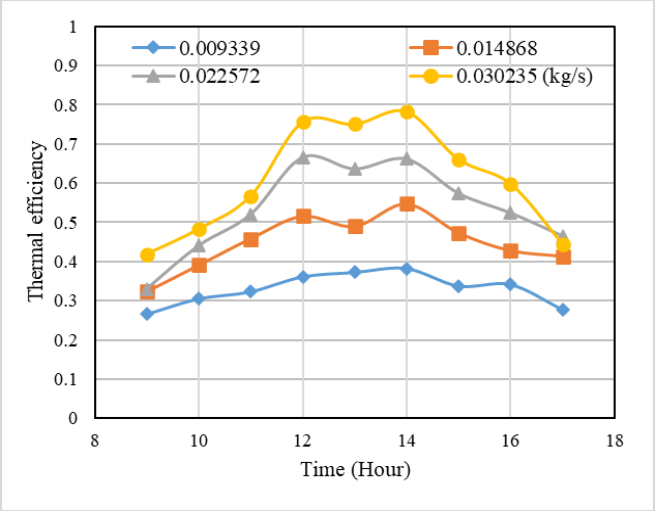

Figure 10: Time-dependent variation of thermal efficiency with PCM in March

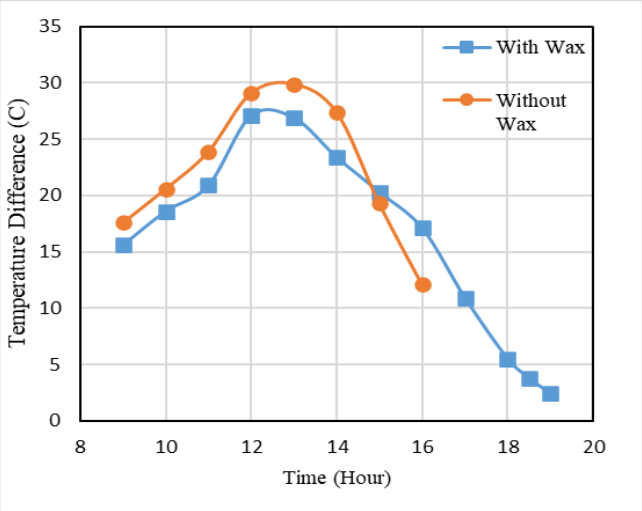

Figure 11: The temperature difference variation with time with and without wax at 0.018686 kg/s

Also, the figure shows that the charging period begins from 9 am to 3 pm, and the temperature rises steadily during the charging period until all the wax melts. During the discharge, the wax temperature was higher than the surface temperature of the absorber. Integrating thermal energy storage systems directly with the microchannels improved the performance of the solar concentrator. Also, to increase the efficiency of these energy-storing materials, PCM material inside the tank contains pin fins to enhance thermal conductivity, and the fins inside the wax speed up the heat exchange process.This work doesn't conform with

previous works, so the results compared with the closest research, a flat plate microchannel air collector, is shown in Figure 12. The figure shows that the efficiency of the current work is higher than Jalil and Abdulkadhim [16] despite the smallness of the absorbing plate for the current work compared to Jalil and Abdulkadhim [16]. This is due to the use of the solar concentrator, which intensifies the radiation, and the dual-axis solar tracking.

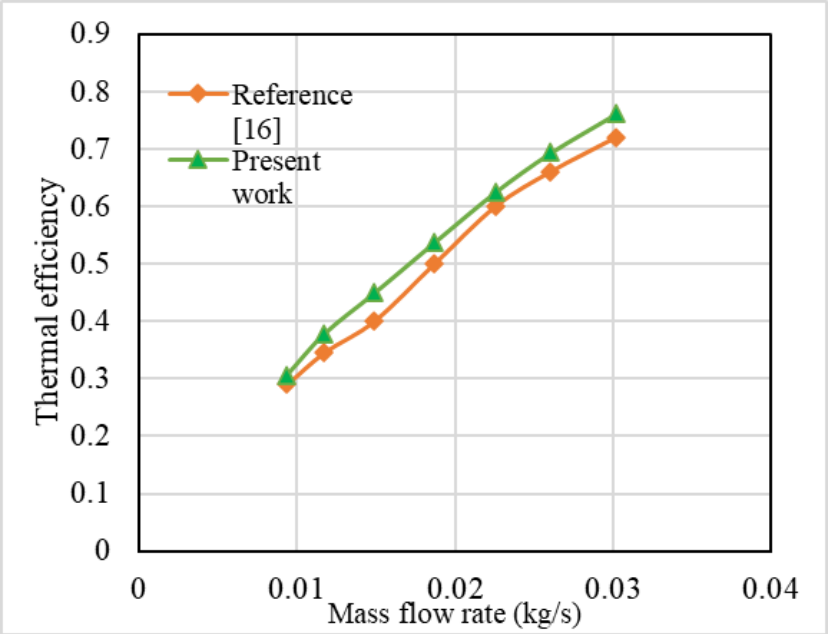

Figure 12: Comparison between the present work and flat plate solar air collector with microchannel [16]

7. Conclusion

Because PCMs can absorb and release heat as needed, they are useful in many industries, including solar collectors. PCM can also match the energy supply and demand components to meet the demands for cooling. Numerous intriguing microchannel layouts have been developed in recent decades. A microchannel is a technique that minimizes the dimensions to break the boundary layer so the heat can reach the core of the microchannel and thus get a high heat transfer coefficient (h). A new design was used for the receiver and reflector in the parabolic solar concentrator; the receiver consists of multiple layers of small channels, and the reflector is designed to focus the solar radiation on two sides. The solar concentrator system is attached to the tracking system, which is put together to move the concentrator according to data from the sensors to maintain the parabolic collector's constant perpendicularity to the sun.

The result indicated that

1) The two-axis tracking system would increase thermal efficiency.
2) Maximum temperature difference occurs between 12:00 and 1:00 pm due to increases in solar intensity.
3) The inverse relationship between the air flow rate and the air temperature difference.
4) The maximum energy storage period was 3 hours.
5) The thermal efficiency is 54.98% in January, 69.3% in March, and 80.9% in July at the flow rate of 0.026064 kg/s.

Nomenclature

q	Heat gain (W)
$\dot{m}$	Mass flow rate (kg/s)
T_{out} , T_{in}	Outlet and inlet air temperature (K)
I	Solar radiation (W/m^2)
ρ	Air density (kg/m^3)
K	Thermal conductivity (W/m K)
η_{th}	Thermal efficiency
$\emptyset_r$	Rim angle
A_a	Aperture Ares
A_r	Received Area
W_a	Aperture width,
C_P	Specific heat, kJ/kg°C.
T_m	PCM's melting point,°C

Author contributions

Conceptualization, J. Hamdi. J. Jalil and A. Reja; writing—original draft preparation, J. Hamdi. J. Jalil and A. Reja.; writing—review and editing, J. Hamdi. J. Jalil and A. Reja.; supervision, J. Jalil and A. Reja. All authors have read and agreed to the published version of the manuscript.

Funding

This research received no specific grant from any funding agency in the public, commercial, or not-for-profit sectors.

Data availability statement

The data that support the findings of this study are available on request from the corresponding author.

Conflicts of interest

The authors declare that there is no conflict of interest.

Reference

[1] N. I. Dawood, J. M. Jalil, and M. K. Ahmed, Investigation of a novel window solar air collector with 7-moveable absorber plates, Energy, 257 (2022) 124829. https://doi.org/10.1016/j.energy.2022.124829

[2] J. M. Jalil, M. K. Ahmed, and H. A. Idan, Experimental and Numerical Study of a New Corrugated and Packing Solar Collector, IOP Conf. Ser. Mater. Sci. Eng., 765, 2020,012026. https://doi.org/10.1088/1757-899X/765/1/012026

[3] A. A. Eidan, A. AlSahlani, A. Q. Ahmed, M. Al-faham, and J. M. Jalil, Improving the performance of heat pipe-evacuated tube solar collector experimentally by using Al_2O_3 and CuO/acetone nanofluids, Sol. Energy, 173 (2018) 780–788. https://doi.org/10.1016/j.solener.2018.08.013

[4] F. S. Javadi, H. S. C. Metselaar, and P. Ganesan, Performance improvement of solar thermal systems integrated with phase change materials (PCM), a review, Sol. Energy, 206 (2020) 330–352. https://doi.org/10.1016/j.solener.2020.05.106

[5] R. Elbahjaoui and H. El Qarnia, Performance evaluation of a solar thermal energy storage system using nanoparticle-enhanced phase change material, Int. J. Hydrogen Energy, 44 (2019) 2013–2028. https://doi.org/10.1016/j.ijhydene.2018.11.116

[6] S. Ali and S. P. Deshmukh, An overview: Applications of thermal energy storage using phase change materials, Mater. Today Proc., 26 (2019) 1231–1237. https://doi.org/10.1016/j.matpr.2020.02.247

[7] P. S. Lee, S. V. Garimella, and D. Liu, Investigation of heat transfer in rectangular microchannels, Int. J. Heat Mass Transf., 48 (2005) 1688–1704. https://doi.org/10.1016/j.ijheatmasstransfer.2004.11.019

[8] J. Li and G. P. Peterson, 3-Dimensional numerical optimization of the silicon-based high-performance parallel microchannel heat sink with liquid flow, Int. J. Heat Mass Transf., 50 (2007) 2895–2904. https://doi.org/10.1016/j.ijheatmasstransfer.2007.01.019

[9] J. M. Jalil, G. A. Aziz, and A. A. Kadhim, Heat Transfer Enhancement in Air Duct Flow by Micro-Channel Experimental and Numerical Investigation, IOP Conf. Ser. Mater. Sci. Eng., 765, 2020. https://doi.org/10.1088/1757-899X/765/1/012027

[10] J. M. Jalil, A. H. Reja, and A. M. Hadi, Numerical Investigation of Thermal Performance of Micro-Pin Fin with Different Arrangements, IOP Conf. Ser. Mater. Sci. Eng., 765, 2020. https://doi.org/10.1088/1757-899X/765/1/012037

[11] F. O. Al Ghuol, K. Sopian, and S. Abdullah, Enhancement of integrated solar collector with spherical capsules PCM affected by additive aluminium powder, J. Thermodyn., 2016, https://doi.org/10.1155/2016/1604782

[12] T. K. Murtadha, H. M. Salih, and A. D. Salman, Experimental and Numerical Study of Closed Loop Solar Chimney Assisted with PCM and CFM as Thermal Energy Storage Collector, Eng. Technol. J., 34 (2016) 2450–2463. https://doi.org/10.30684/etj.34.13a.8

[13] A. H. Abed, Thermal Storage Efficiency Enhancement for Solar Air Heater Using a Combined SHS, Eng. Technol. J., 34 (2016) 999–1011.https://doi.org/10.30684/etj.34.5A.16

[14] D. Yang, Z. Jin, Y. Wang, G. Ding, and G. Wang, Heat removal capacity of laminar coolant flow in a microchannel heat sink with different pin fins, Int. J. Heat Mass Transf., 113 (2017) 366–372. https://doi.org/10.1016/j.ijheatmasstransfer.2017.05.106

[15] I. A. Ghani, N. Kamaruzaman, and N. A. C. Sidik, Heat transfer augmentation in a microchannel heat sink with sinusoidal cavities and rectangular ribs, Int. J. Heat Mass Transf., 108 (2017) 1969–1981. https://doi.org/10.1016/j.ijheatmasstransfer.2017.01.046

[16] J. M. Jalil and N. A. Abdulkadhim, Effect of micro-channel technique on solar collector performance, IOP Conf. Ser. Mater. Sci. Eng., 518, 2019, https://doi.org/10.1088/1757-899X/518/3/032047

[17] M. Mofijur et al., Phase change materials (PCM) for solar energy usages and storage: An overview, Energies, 12, 2019. https://doi.org/10.3390/en12163167

[18] C. V. Podara, I. A. Kartsonakis, and C. A. Charitidis, Towards phase change materials for thermal energy storage: classification, improvements and applications in the building sector, Appl. Sci., 11 (2021) 1–26. https://doi.org/10.3390/app11041490

[19] A. Kushwah, M. Kumar Gaur, and R. Kumar Pandit, The Role of Phase Change Materials for Lifetime Heating of Buildings in Cold Climatic Conditions, Int. J. Built Environ. Sustain., 7 (2020) 81–96. https://doi.org/10.11113/ijbes.v7.n3.600

[20] A. Nematpour Keshteli and M. Sheikholeslami, Nanoparticle enhanced PCM applications for intensification of thermal performance in building: A review, J. Mol. Liq., 274 (2019) 516–533. https://doi.org/10.1016/j.molliq.2018.10.151

[21] S. Dabiri, M. Mehrpooya, and E. G. Nezhad, Latent and sensible heat analysis of PCM incorporated in a brick for cold and hot climatic conditions, utilizing computational fluid dynamics, Energy, 159 (2018) 160–171. https://doi.org/10.1016/j.energy.2018.06.074

[22] X. Chen, P. Cheng, Z. Tang, X. Xu, H. Gao, and G. Wang, Carbon-Based Composite Phase Change Materials for Thermal Energy Storage, Transfer, and Conversion, Adv. Sci., 8 (2018) 1–38. https://doi.org/10.1002/advs.202001274

[23] A. Kumar, Mathematical Modeling and Optimization of a Parabolic Trough Concentrator for the Improvement of Collection Efficiency, Int. J. Innovative Res. Eng. Manag., 3 (2016) 375-380.

[24] Cengel, Y. A., Heat Transference a Practical Approach, MacGraw-Hill, 2004.